Vapor Deposition of Silicon-Containing

Microstructured Polymer Films onto Silicone Oil

Substrates

Authors: Nicholas A. Welchert, Bryan Nguyen, Theodore T. Tsotsis, and Malancha Gupta*

Mork Family Department of Chemical Engineering and Materials Science, University of

Southern California, 925 Bloom Walk, Los Angeles, California 90089, United States

ABSTRACT

In this study, a silicon-containing crosslinked polymer, poly(1,3,5,7-tetravinyl-1,3,5,7-tetramethylcyclotetrasiloxane-co-ethylene glycol diacrylate) (p(V4D4-co-EGDA)), was deposited onto high viscosity silicone oil using initiated chemical vapor deposition (iCVD). The ratio of the feed flow rate of V4D4 to EGDA was systematically studied and the chemical composition and morphology of the top and bottom surfaces of the films were analyzed. The films were microstructured and the porosity and thickness of the films increased with increasing V4D4 content. The top of the film was comprised of densely-packed and loosely-packed microstructured regions. X-ray photoelectron spectroscopy on the top and bottom surfaces of the films showed a heterogeneous chemical composition along the thickness of the film, with higher silicon content on the top surface compared to the bottom surface. To our knowledge, this is the first study of iCVD deposition of a silicon-containing polymer films onto silicone oil. The results of this study can be used for the synthesis of polymer precursors films for the fabrication, via pyrolysis, of

silicon-based inorganic membranes for use in hydrogen production using silicone oil to prevent infiltration of monomer into the underneath membrane support structure during vapor deposition.

Introduction

Silicon-based porous asymmetric inorganic membranes have been shown to have excellent hydrogen separation properties^{1,2,3} and are, thus, ideal for use in hydrogen production through catalytic methane steam reforming and biomass or coal gasification. In comparison to their polymer counterparts, these membranes have been shown to be stable at high temperatures and pressures and can withstand the corrosive environments that are involved in hydrogen production. Such inorganic membranes are often fabricated by the application of a pre-ceramic silicon-containing polymer film on a mechanically strong porous ceramic substrate and its subsequent pyrolysis. A uniform polymer film on top of the porous substrate is ideal for the formation of high-quality ceramic membranes. The dense polymer film deposition methods to date, typically, employ solvent-based techniques, such a slip-casting¹⁰, spin-coating^{11,12}, and dipcoating¹³, which use potentially environmentally harmful solvents such as toluene, benzene, and tetrahydrofuran.

The development of vapor phase polymer deposition methods for the fabrication of preceramic silicon-containing polymer films shows promise for reducing solvent use. In particular, the iCVD method is a solvent-free polymerization technique that is traditionally used to deposit thin films on a variety of solid substrates. ^{14,15,16} In this process, monomer and initiator vapors are introduced into a vacuum chamber where the initiator is thermally cleaved by a heated filament array to produce free radicals. The monomer molecules and initiator radicals adsorb onto the

surface of a substrate where polymerization occurs via a free-radical mechanism, producing a dense film. Tert-butyl peroxide (TBPO) is, typically, used as the initiator.¹⁷ We recently used iCVD to deposit a crosslinked silicon-containing polymer poly(1,3,5,7-tetravinyl-1,3,5,7-tetramethylcyclotetrasiloxane) (pV4D4) onto a macroporous support and subsequently pyrolyzed the film to form a silica membrane.¹⁸ These asymmetric membranes utilized a macroporous silicon carbide (SiC) substrate with a mesoporous SiC top layer, prepared via the dipcoating and subsequent pyrolysis of a pre-ceramic polymer film, in order to prevent infiltration, during polymerization, of the pV4D4 polymer into the macroporous substrate, which would then result in clogging of the pores and waste of the monomer and initiator precursors.⁶

In this paper, we study for the first time the iCVD deposition of silicon-containing polymer films onto low surface tension, high viscosity silicone oils, serving the same role as the SiC mesoporous scaffolds confining the polymer film growth on the top of the macroporous substrates, and thus avoiding infiltration during the preparation of asymmetric inorganic membranes. Our group has previously shown that the iCVD process can, indeed, be used to deposit other types of polymers onto low vapor pressure liquid substrates, such as ionic liquids and silicone oils. ^{19,20,21} The surface tension interactions between the deposited polymer and the liquid substrate determine whether a dense polymer film²² or polymer particles^{23,24} form, the latter being an undesirable outcome when preparing inorganic membrane and sensor films.

In this paper, we systematically investigate the iCVD deposition of copolymer poly(1,3,5,7-tetravinyl-1,3,5,7-tetramethylcyclotetrasiloxane-co-ethylene glycol diacrylate) (p(V4D4-co-EGDA)) films, and study their properties as a function of their V4D4 content. For this study, the ratio of the V4D4 to the EGDA feed flow rates into the iCVD reactor was systematically varied,

and the resulting chemical composition and morphology of the top and bottom surfaces of the polymer film were analyzed. The crosslinker EGDA was used because the deposition of a homopolymer pV4D4 film on the silicone oil surface at typical reactor conditions did not result in film formation. The results of this study can be used to guide future research into the fabrication of silicon-based inorganic membranes for use in hydrogen production, employing silicone oil as an easy-to-apply barrier to reduce pre-ceramic polymer infiltration into the underlying macroporous supports.

Experimental Section

Silicone oil (1000 centistokes (cSt), Sigma-Aldrich), 1,3,5,7-tetravinyl-1,3,5,7-tetramethylcyclotetrasiloxane (V4D4) (Gelest, Inc.), ethylene glycol diacrylate (EGDA) (97% MonomerPolymer), tert-butyl peroxide (TBPO) (98% Sigma-Aldrich), and hexane (98% VWR) were all used as received. All polymer film depositions were performed using a custom-designed pancake-shaped iCVD vacuum chamber that is 250 mm in diameter and 48 mm in height (GVD Corporation). For polymer film depositions onto liquid, 0.5 mL of 1000 cSt silicone oil was pipetted onto a silicon wafer (Wafer World, 100 mm). The silicon wafers were then placed on the reactor stage that was maintained at a constant temperature using a recirculating chiller (Thermo Scientific NESLAB RTE 7). A nichrome filament array (Omega Engineering, 80%/20% Ni/Cr) inside the reactor was heated during the deposition process to thermally decompose the TBPO initiator. The reactor pressure was maintained using a throttle valve (MKS 153D) and measured using a capacitance manometer (MKS Baratron 622A01TDE). The V4D4 and EGDA flow rates were metered using a needle valve. The TBPO flow rate was metered using a mass flow controller (MKS 1479A), and was maintained at 1 standard cubic centimeters per minute (sccm) for all

experiments. The polymer deposition rates were monitored on a reference silicon wafer using an in situ 633 nm helium—neon laser interferometer (Industrial Fiber Optics). Table 1 lists the reactor conditions for each sample.

A quartz crystal microbalance (QCM) (Sycon Instruments) with a 6 MHz gold-plated crystal was used to compare the adsorption of the precursor onto a bare gold crystal versus the adsorption and absorption of the precursor when a thin layer of 1000 cSt silicone oil is added to the crystal. A glass pipette was used to transfer silicone oil onto the gold crystal before being placed within the reactor and the oil was allowed to slowly spread over time to cover the entire surface of the crystal. Before experimentation, the microbalance was zeroed out in order to account for the addition of the silicone oil when compared to the bare gold crystal. The experiments were performed at pressures, temperatures, and flow rates consistent with the range of deposition conditions. The uptake of each precursor (V4D4, EGDA, and TBPO) was studied independently of each other. The mass uptake of each precursor was allowed to equilibrate, which occurred within 2 minutes. The presence of absorption was determined by measuring the difference in mass uptake of the precursor on the bare gold crystal versus the gold crystal with a thin layer of silicone oil on the top of it.

The chemical composition of the deposited polymer films on the reference silicon wafers was analyzed using Fourier transform infrared (FTIR) spectroscopy (Nicolet iS10, Thermo Scientific). 32 scans were collected between 4000 and 500 cm⁻¹ with a resolution of 4 cm⁻¹. In order to confirm the chemical composition of the films deposited on the silicone oil, X-ray photoelectron spectroscopy (XPS) survey scans of the removed copolymer films were taken at both the top and bottom surfaces of the films. A Kratos Axis Ultra DLD XPS spectrometer equipped with a magnetic immersion lens, a charge neutralization system, and a monochromator

Al X-ray source was used to collect the survey spectra. Survey spectra were taken from 800 eV to 0 eV in 1 eV steps and averaged over seven scans. All XPS survey spectra are shown in the Supporting Information document (Figure S1-S17). The XPS data were analyzed using the software CasaXPS. The copolymer films were removed from the liquid after deposition by placing the sample in a hexane bath for 15 minutes to separate the film from the silicone oil. The films were then cut into two samples and were either left on the silicon wafer having the top surface exposed or removed from the silicon wafer and placed on a separate clean silicon wafer, using carbon tape as an adhesive, with the bottom surface exposed. Once the samples were mounted, they were soaked in hexane for another 15 minutes to remove any residual silicone oil. The samples were then removed from the hexane bath and placed into a vacuum chamber at room temperature for 12 hours. The morphology of the cross-section, top, and bottom surfaces of the films was imaged by scanning electron microscopy (SEM) (JEOL-4500) using a 25 kV acceleration voltage (SE detection mode). Prior to imaging, the samples were sputter-coated for 60 s at 40 mA with gold in order to prevent charging. The ImageJ software (version 1.53m, National Institutes of Health, Bethesda, MD) was used to determine the surface porosity of the top and bottom of the films deposited on silicone oil. Table TS1 in the Supporting Information document reports the average porosity and corresponding standard deviation values derived from SEM images of three separate locations on the films. Similarly, Table TS2 in the same document reports the average microstructure pore size and standard deviation of the top of the films, once more determined using the ImageJ software.

Results and Discussion

For our studies, we used 1000 cSt silicone oil as our substrate. The absorption of monomer molecules in the liquid substrate has been shown to affect the morphology of the deposited polymer. 25,26 A QCM was used in this research to study 1,3,5,7-tetravinyl-1,3,5,7tetramethylcyclotetrasiloxane (V4D4), ethylene glycol diacrylate (EGDA), and tert-butyl peroxide (TBPO) absorption in the silicone oil at the relevant reactor conditions. We have previously shown^{24,27} that QCM measurements can be used as an indicator of whether a certain precursor only adsorbs on the surface of a liquid substrate versus absorbing in its bulk. By first measuring the mass uptake on a bare gold surface and then on the same surface coated by a thin layer of liquid, one can readily distinguish whether only adsorption versus absorption takes place,²⁷ since in the former case the mass uptakes are quite similar and the adsorbed amounts on a bare gold surface and on a liquid-coated gold surface are, typically, close to each other. Significant differences in the mass uptakes measured, on the other hand, offer strong indication that absorption does, indeed, take place. The measured mass uptakes of V4D4, EGDA and TBPO on a bare gold surface were 0.060, 0.044, and 0.016 µg/cm², respectively. After applying a thin layer of 1000 cSt silicone oil to the gold crystal before placement into the reactor, the corresponding mass uptakes of V4D4, EGDA and TBPO were 6.282, 0.049, and 0.012 µg/cm², respectively. The mass uptakes of EGDA and TBPO with and without silicone oil are similar, likely indicating that there is no absorption in the silicone oil, whereas the significant increase in V4D4 mass uptake in the presence of silicone oil indicates that there is V4D4 absorption in the silicone oil. Since the V4D4 monomer absorbs and is soluble in the silicone oil, it would be unlikely that one could identify reactor conditions under which a homopolymer pV4D4 film would form at the surface of the silicone oil.

Since the QCM tests indicated that the EGDA monomer does not absorb in the silicone oil and remains instead on the surface of the liquid, we investigated whether copolymerizing EGDA and

V4D4 would help lead to the formation of p(V4D4-co-EGDA) films on the surface of the silicone oil. In these experiments, we systematically varied the ratio (*r*) of the reactor feed flow rate of V4D4 to that of EGDA from 1:1.5 to 1:1 and finally to 1.5:1 in order to prepare three different samples A, B, and C, as described in Table 1. All experiments maintained a constant TBPO flow rate of 1 sccm and a filament temperature of 250 °C throughout deposition. All three different feed flow rate ratios resulted in the deposition of a thin polymer film on the surface of the silicone oil. These results are consistent with our previous work²⁸ which has shown that EGDA can be used as a cross-linker for the deposition onto silicone oil of copolymer films, poly(2-hydroxyethyl methacrylate-co-ethylene glycol diacrylate) and poly(1-vinyl-2-pyrrolidone-co-ethylene glycol diacrylate).

Table 1. Deposition conditions for the various samples.

| Sample | V4D4 Flow Rate (sccm) | EGDA Flow Rate (sccm) | V4D4:EGDA Flow Ratio (r) | Stage Temperature (°C) | Reactor Pressure (mTorr) | Deposition Rate $(\frac{nm}{min})$ |
|--------|-----------------------------|-----------------------------|--------------------------------|------------------------------|--------------------------------|------------------------------------|
| A | 0.4 | 0.6 | 1:1.5 | 40 | 75 | 4.2 |
| В | 0.4 | 0.4 | 1:1 | 40 | 110 | 4.7 |
| C | 0.6 | 0.4 | 1.5:1 | 40 | 110 | 4.2 |
| D | - | 0.4 | - | 40 | 55 | 4.6 |
| E | 0.5 | - | - | 40 | 190 | 10 |

To keep the mass of polymer deposited on the liquid surface consistent among the three different samples prepared, the polymerization reaction was allowed to proceed until a 400 nm thick film, measured in situ by laser interferometry, was deposited on a reference silicon wafer placed in the same reactor. A control deposition of homopolymer pEGDA onto the silicone oil was also conducted (sample D), which resulted in the formation of a thin polymer film on the surface of the silicone oil. A control deposition of a dense pV4D4 (Sample E) film on a silicon wafer was also carried out in order to create references of the bulk homopolymer as it does not form a film on silicone oil under all reactor conditions we investigated. To determine the chemical composition

of the copolymer films, Fourier transform infrared (FTIR) analysis was conducted on the films deposited on reference silicon wafers and the spectra were compared to the homopolymer pV4D4 and homopolymer pEGDA films also deposited on reference silicon wafers. As shown in Figure 1, the spectra of the three different copolymer films (A, B, and C, see Table 1) contain the characteristic C=O bond peak at 1735 cm⁻¹, which indicates the presence of EGDA; in addition, all three spectra contain the characteristic Si-O-Si peak at 1065 cm⁻¹, which indicates the presence of V4D4, thus confirming copolymerization. The ratio of the intensity of the Si-O-Si peak to that of the C=O peak in samples A, B, and C is equal to 0.6, 0.9, and 1.2, respectively, thus indicating an increase in the fraction of V4D4 incorporated into the copolymer films as the feed flow rate ratio of V4D4 to that of EGDA increases.

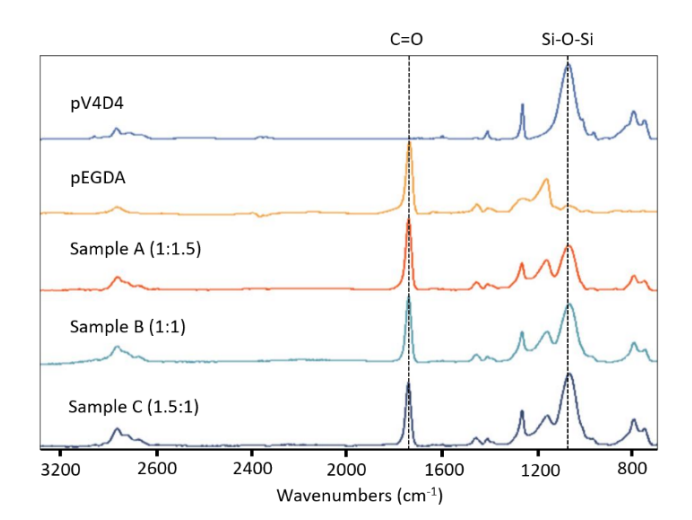


Figure 1. FTIR spectra of pV4D4 and pEGDA films and of copolymer films deposited on reference wafers placed in the reactor during deposition of samples A, B, and C; dashed lines indicate the position of the C=O and Si-O-Si peaks

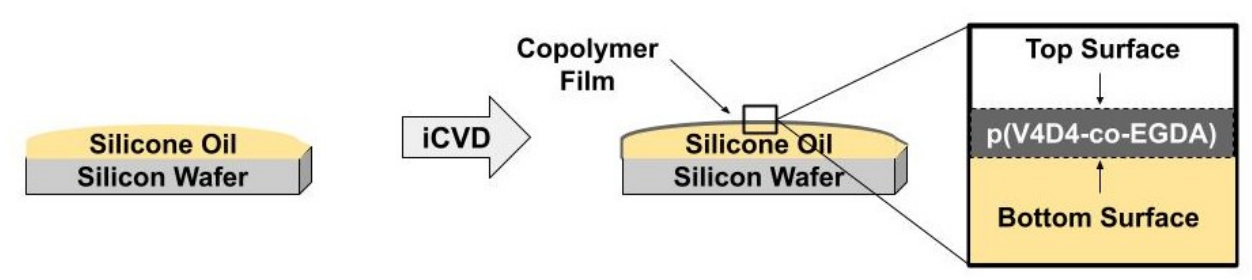


Figure 2. Schematic depicting the top and bottom surfaces of the p(V4D4-co-EGDA) film deposited onto silicone oil.

The chemical composition of the top and bottom surfaces of the copolymer films deposited on the silicone oil, as shown in Figure 2, were analyzed via X-ray photoelectron spectroscopy (XPS, and the XPS survey spectra can be found in the Supporting Information document (Figure S1-S11). The copolymer films were easily prone to cracking, indicating a lack of mechanical strength. Therefore, to further study their properties, following deposition, the films were placed in a hexane bath to remove the silicone oil and were then either left on the silicon wafer with the top surface exposed or carefully removed, placed on a separate clean silicon wafer, using carbon tape as an adhesive, with the bottom surface exposed. Both samples were then dried under vacuum at room temperature. As shown in Table 2, there is an increase in the silicon content both at the top and bottom surfaces of the film as the V4D4 flow rate increases relative to the EGDA flow rate. This indicates greater incorporation of V4D4 into the copolymer, consistent with the FTIR data of the films deposited on the reference silicon wafers. It should be noted that use of hexane²⁹ and high viscosity liquids,30 such as silicone oil,31 with samples prior to XPS can have an effect on the resulting spectrum. In order to confirm the observed silicon content trends among samples A, B, and C, the reference wafers, in which no solvents or high viscosity liquids were used, from each deposition were also analyzed (Table 2). The same trends observed on the top and bottom surfaces of the film are also observed on the reference wafers, indicating the hexane and the silicone oil do not affect the observable trends in the copolymer films deposited on the liquid. It is also observed that for all samples deposited on liquid, the silicon content at the top surface is greater than the content at the bottom surface. Since V4D4 does not polymerize into a thin film at typical reaction conditions due to the fact that it absorbs into the silicone oil the copolymer films are likely formed by the EGDA first polymerizing on the surface of the liquid to form a base layer before its reaction with V4D4 commences. This copolymer film formation mechanism is consistent with the observed nonuniform chemical composition along the thickness of the film, see Table 2, with less incorporation of V4D4 found at the bottom surface. As the silicon content is higher on the top surface and lower on the bottom surface than that of the reference wafers for all samples, it is also noted as an observable trend that is not affected by hexane and silicone oil. The ratio of carbon, oxygen, and silicon reported on the reference wafer, sample B, is also consistent with the expected values for an equal composition copolymer. As the silicon content on the top surface of the films is higher for each sample compared to that of their corresponding reference wafer it should be noted that the composition ratio trends for these samples are consistent with the reference wafer trends. However, the same trend in ratios does not occur for the bottom surface, likely due to the use of carbon tape as an adhesive to the silicon wafer.

Table 2. XPS atomic composition of the top and bottom surfaces of the p(V4D4-co-EGDA) films deposited on silicone oil.

Atomic Composition (%)

| Sample | Carbon | Oxygen | Silicon |
|--------|----------------|---------------|-----------|
| | | Top Surface | |
| A | 68.92 | 18.02 | 13.69 |
| В | 58.95 | 23.96 | 17.09 |
| C | 54.99 | 25.57 | 19.44 |
| | Bottom Surface | | <u>e</u> |
| A | 67.67 | 24.78 | 7.55 |
| В | 71.99 | 19.75 | 8.25 |
| C | 68.62 | 20.87 | 10.51 |
| | <u>R</u> | eference Wafe | <u>rs</u> |

| A | 68.02 | 22.89 | 9.09 | | |
|-------|-------|-----------------------|-------|--|--|
| В | 61.21 | 25.16 | 13.63 | | |
| C | 57.07 | 27.73 | 15.20 | | |
| | Refer | Reference Homopolymer | | | |
| pEGDA | 65.63 | 30.5 | 3.87 | | |
| pV4D4 | 50.51 | 26.19 | 23.3 | | |

Scanning electron microscopy (SEM) was used to visualize the bottom surface of the pEGDA and p(V4D4-co-EGDA) films, which are all composed of microstructures (see top-down images in Figure 3). Our previous work²⁸ has shown that homopolymer pEGDA films formed on silicone oils of various viscosities via iCVD deposition are characterized by similar microstructures; we speculated in the earlier study that this is due to chemical cross-linking which helps to form polymer networks. The microstructures grow by simultaneous polymer diffusion and aggregation and wetting of the growing aggregates by the liquid. Our previous work on the use of various liquid viscosities has shown that higher viscosity liquids result in slower diffusion and aggregation of the wetted polymer regardless of the polymer and liquid used, 22,24 leading to more dense microstructured pEGDA films like the one shown in Figure 3. The bottom surfaces of all three p(V4D4-co-EGDA) films (Sample A, B, and C) appear highly porous, characterized by threedimensional structures; the porosity and three-dimensional character of the film both increase as the content of V4D4 in the copolymer increases relative to EGDA. The increase in porosity, determined via the ImageJ software, is reported in Table TS1 in the Supporting Information document. The morphology of the copolymer films is, in fact, similar to that observed in our previous study with pEGDA films deposited on lower viscosity silicone oils (5-500 cSt).²⁸ In that case, lower viscosity liquids cause greater diffusion and aggregation of the wetted polymer, leading to more porous films. The impact that V4D4 has on the characteristics of the polymer films formed may suggest, therefore, that the incorporation of V4D4 increases polymer diffusion. We

hypothesize that the increase in polymer diffusion is likely due to the chemical similarity of V4D4 which also explains its solubility in the silicone oil. Work by Kim et al.³¹ has shown that the extent of polymer dissolution and diffusion in silicone oil can be deduced from comparing the solubility parameters between the two substances. When the difference between the solubility parameters of two compounds is less than 3.5-4.5, then dissolution and diffusion of one compound into another is likely to occur. The Hildebrand solubility parameters (MPa^{1/2}) for V4D4, EGDA, and silicone oil are reported³² to be 12.3, 19.2, and 14.0, respectively, indicating that the V4D4 is likely to dissolve and diffuse in the oil while EGDA will not.

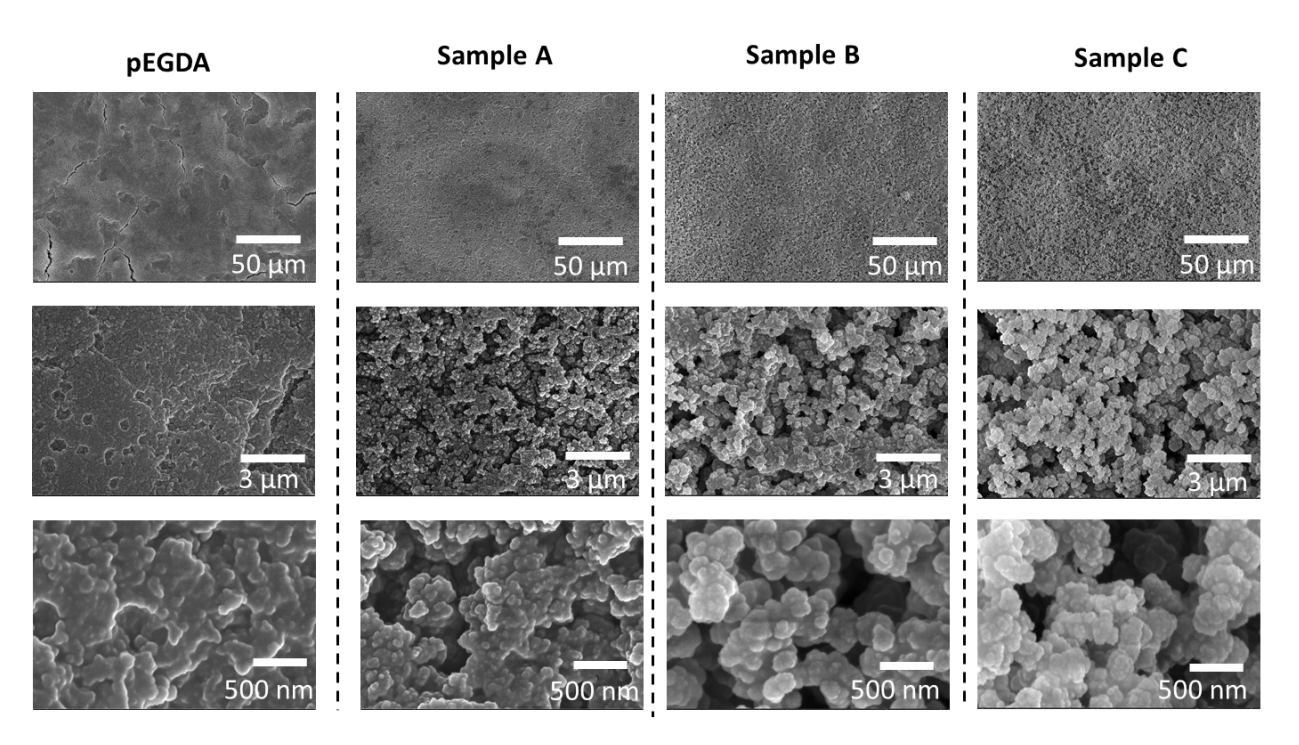


Figure 3. Top-down SEM images of the bottom surface of the pEGDA film and copolymer films (samples A, B, and C) deposited onto 1000 cSt silicone oil.

SEM images of the top surface of the pEGDA and the copolymer films were also taken. Both the pEGDA and copolymer films are macroscopically non-uniform with both densely-packed and

loosely-packed microstructured regions (an example for the copolymer case is shown in Figure 4). For the copolymer films, the densely-packed regions are characterized by larger size microstructures with lower porosity and three-dimensional character relative to the loosely-packed regions. Microstructure size and porosity, determined via the ImageJ software, are both reported in the Supporting Information document (Tables TS1-TS2). Figure 5 shows images of the denselypacked regions for both the pEGDA and the copolymer films. The densely-packed region for pEGDA is a completely dense, non-porous film. As more V4D4 is incorporated in the copolymer, the densely-packed regions of the films become more porous and have distinct, larger size microstructures. The increase in the microstructure size and porosity of the film, as the V4D4 content in the polymer increases relative to EGDA, is likely due to an increase in polymer diffusion and aggregation at higher concentrations of V4D4, consistent with the trend found on the bottom of the film. Figure 6 shows images of the loosely-packed regions for both the pEGDA and the copolymer films. For the copolymer films these regions are characterized by a higher porosity, more prominent three-dimensional nature, and smaller size microstructures relative to the denselypacked regions. As more V4D4 is incorporated into the copolymer, the porosity, three-dimensional nature, and microstructure size of the loosely-packed regions of the films all increase, similarly to the behavior shown by the densely-packed regions.

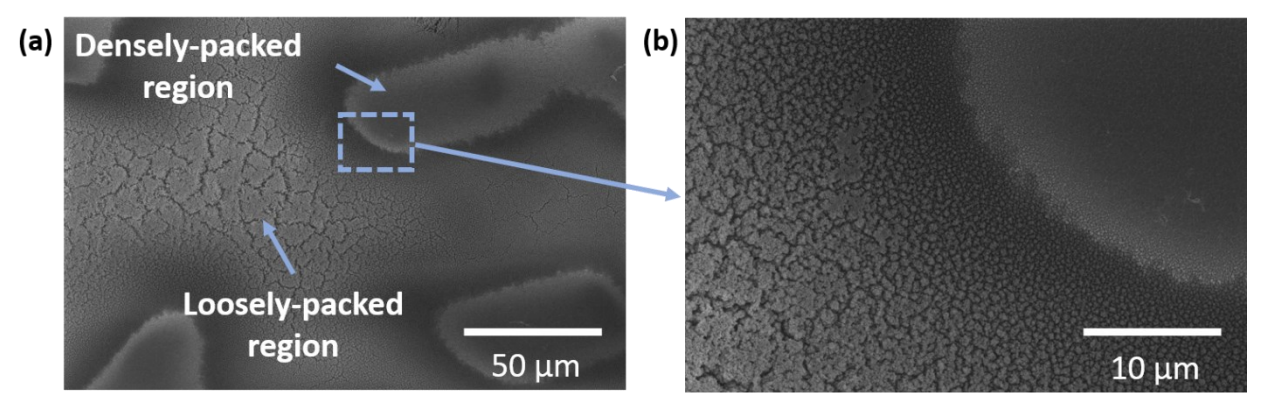


Figure 4. (a) SEM image of the top surface of the p(V4D4-co-EGDA) film (Sample A) showing an example of the densely-packed and loosely-packed regions. (b) Higher magnification image of the interface between the densely-packed and loosely-packed regions.

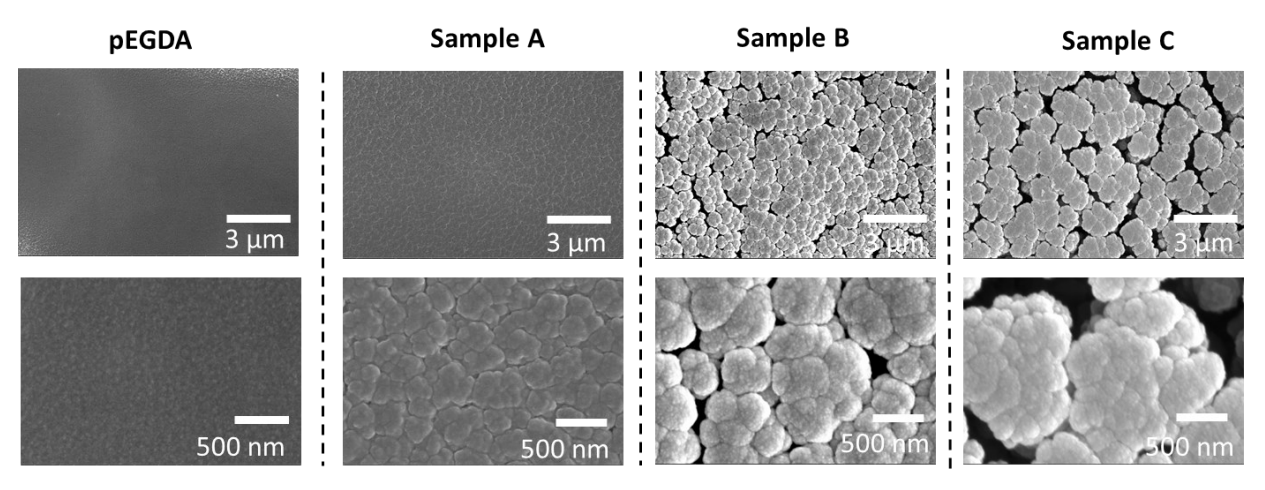


Figure 5. SEM images of the densely-packed regions of the top surface of the pEGDA film and copolymer films (samples A, B, and C) deposited onto 1000 cSt silicone oil.

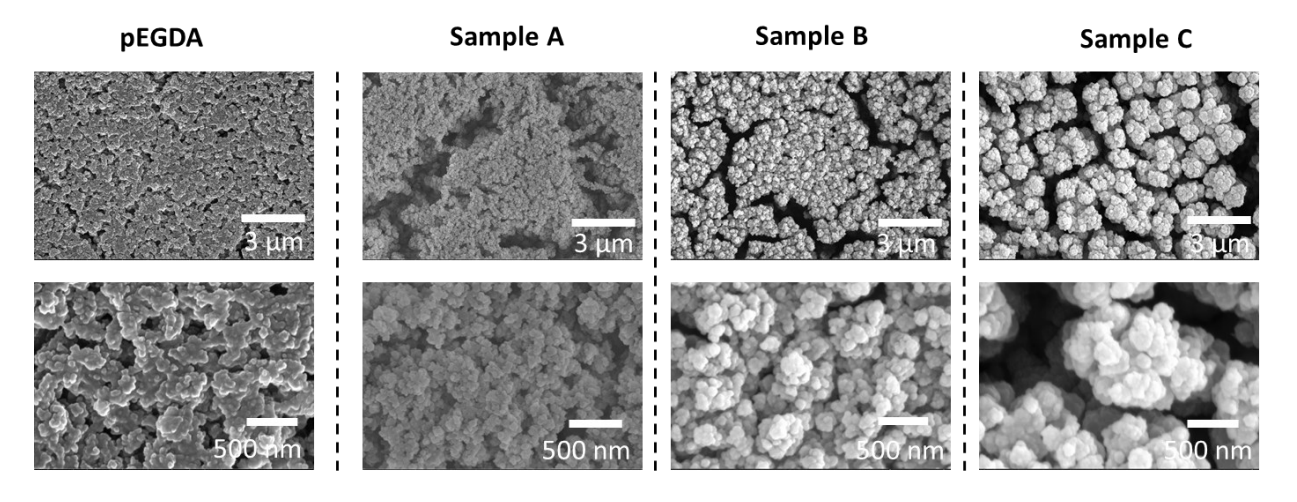


Figure 6. SEM images of the loosely-packed regions of the top surface of the pEGDA film and copolymer films (samples A, B, and C) deposited onto 1000 cSt silicone oil.

SEM images of the cross-sections of the films are shown in Figure 7. The cross-section thickness was measured at three different locations along the length of each film. The corresponding thicknesses of samples A, B, C, and D were 4.0 ± 0.5 , 4.8 ± 0.2 , 6.3 ± 0.3 , and 3.0± 0.1 μm, respectively. The pEGDA has a relatively dense, microstructured cross-section similar to what has been observed in our previous work using high viscosity liquids.²⁸ The thickness of all the p(V4D4-co-EGDA) films is larger than the thickness of the pEGDA film. The cross-sections of the copolymer films have columnar microstructures and increase in thickness as more V4D4 is incorporated into the film, which indicates faster polymer diffusion and aggregation of the wetted polymer, which is consistent with the SEM images of the top and bottom surfaces of the films. In order to observe how reaction time affects the thickness of the films, p(V4D4-co-EGDA) was deposited with a flow rate ratio of 1:1 for three different deposition times of 45, 90, and 120 minutes. As Figure 7b indicates, there is an increase in film thickness as deposition time increases. This indicates that as deposition continues, polymer diffusion, aggregation, and wetting continuously occur throughout the time of deposition, thus creating thicker films. XPS was conducted on the top and bottom surfaces of the three samples generated with different deposition times (see Table 3), and the XPS survey spectra can be found in the Supporting Information document (Figure S12-S17). Similar to samples A, B, and C, see Table 2, the bottom surface showed a lower silicon content than the top side, which again is explained by the fact that the EGDA polymerizes first to form the base layer of the film. The chemical composition of the top surface did not show a similar trend, indicating that deposition time has no effect on the silicon content in the top of the film. We determined that the silicon contents for all three deposition times for the top of the films are within experimental error from each other. These observations imply that once the initial base layer of pEGDA coats the liquid surface, a steady deposition rate of the

copolymer is established, as pEGDA forms a barrier in between the liquid surface and the copolymer films that deposit afterwards.

Table 3. XPS atomic composition of the top and bottom surfaces of the p(V4D4-co-EGDA) films deposited on silicone oil for 45, 90, and 120 minutes at a V4D4 to EGDA flow rate ratio of 1:1.

Atomic Composition (%)

| Deposition Time (min.) | Carbon | Oxygen | Silicon |
|------------------------|----------|---------------|----------|
| | | Top Surface | |
| 45 | 59.83 | 21.83 | 18.34 |
| 90 | 58.95 | 23.96 | 17.09 |
| 120 | 56.16 | 24.42 | 19.42 |
| | <u>]</u> | Bottom Surfac | <u>e</u> |
| 45 | 71.65 | 19.67 | 8.69 |
| 90 | 71.99 | 19.75 | 8.25 |
| 120 | 69.57 | 20.63 | 9.79 |

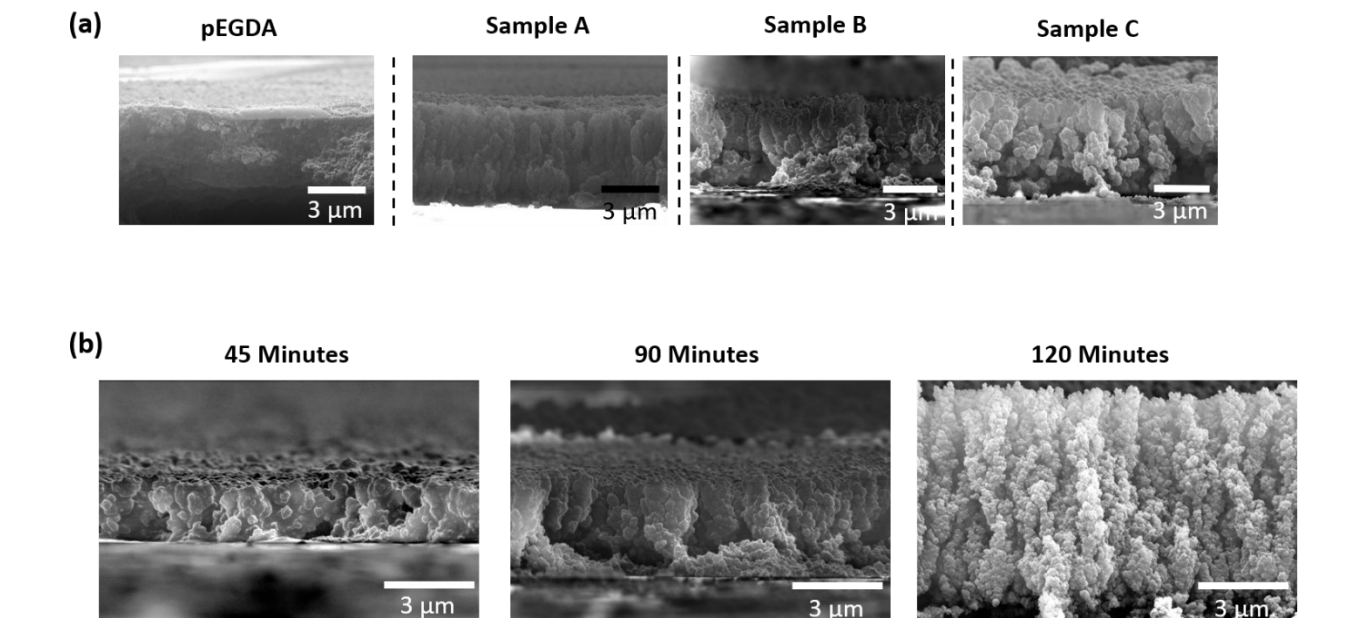


Figure 7. (a) SEM images of the cross-sections of the pEGDA film and copolymer films (samples A, B, and C) deposited onto 1000 cSt silicone oil. (b) SEM images of the cross-section of p(V4D4-co-EGDA) film deposited on 1000 cSt silicone oil for 45, 90, and 120 minutes at a V4D4 to EGDA flow rate ratio of 1:1.

Conclusions

The deposition of p(V4D4-co-EGDA) copolymer films onto 1000 cSt silicone oil via iCVD was systematically studied by varying the flow rates of the two precursor monomers. The morphology and chemical composition of the copolymer films were compared to homopolymer pEGDA films. All the films studied were microstructured. The copolymer films had larger microstructures, higher porosity, and higher thickness compared to the homopolymer pEGDA films, indicating an increase in polymer diffusion and aggregation as V4D4 is incorporated into the film. The films were removed from the liquid surface and SEM was used to visualize the morphology at both their top and bottom surfaces. At the bottom surface of the film, there is greater

porosity and three-dimensional character as the concentration of V4D4 in the copolymer film

increases. At the top surface of the copolymer films, there are both densely-packed and loosely-

packed microstructured regions. As the V4D4 content in the polymer increases, it is observed that

there is an increase in the microstructure size and in porosity of both the densely-packed and

loosely-packed microstructured regions. The cross-sections of all the copolymer films show an

increase in thickness relative to the pEGDA film. XPS analysis showed that the copolymer films

had a higher silicon content at the top surface relative to the bottom surface. This is likely due to

EGDA polymerizing first on the surface of the liquid to form a base layer before reacting with

V4D4, thus resulting in an inhomogeneous chemical composition along the thickness of the film.

As the V4D4 flow rate into the reactor increased relative to the EGDA, an increase in silicon

content at both the top and bottom surfaces of the film was observed. These results indicate that

the flow rate ratio controls the morphology and chemical composition of the copolymer films

formed.

Corresponding Author

*Electronic mail: malanchg@usc.edu

ACKNOWLEDGMENT

This work was supported by the National Science Foundation Award Number CMMI-2012196.

19

REFERENCES

¹ Ockwig, N. W.; Nenoff, T. M. Membranes for hydrogen separation. *Chem. Rev.* **2007**, 107 (10), 4078–4110.

² Elyassi, B.; Sahimi, M.; Tsotsis, T. Inorganic Membranes. In *Encyclopedia of Chemical Processing*; Lee, Sunggyu (K. B.), Ed.; Taylor & Francis Group, LLC: New York, NY, 2009; pp 1-16.

³ Khatib, S. J.; Oyama, S. T.; de Souza, K. R.; Noronha, F. B. Review of Silica Membranes for Separations Prepared by Chemical Vapor Deposition. *Membr. Sci. Technol.* **2011**, 14, 25–60.

⁴ Khalib, N. A. Z.; Daud, F. D. M.; Mel, M.; Hairin, A. L. N.; Azhar, A. Z. A.; Hassan, N. A. Fabrication of Silica Ceramic Membrane via Sol-Gel Dip-Coating Method at Different Nitric Acid Amount Fabrication of Silica Ceramic Membrane via SolGel Dip-Coating Method at Different Nitric Acid Amount. *IOP Conf. Ser. Mater. Sci. Eng.*, **2018**, 290.

⁵ Boffa, V.; Blank, D. H. A.; Elshof, J. E. Hydrothermal Stability of Microporous Silica and Niobia – Silica Membranes. *J. Memb. Sci.* **2008**, 319 (1–2), 256–263.

⁶ Dabir, S.; Deng, W.; Sahimi, M.; Tsotsis, T. Fabrication of Silicon Carbide Membranes on Highly Permeable Supports. *J. Memb. Sci.* **2017**, 537, 239–247.

⁷ Iwamoto, Y.; Sato, K.; Kato, T.; Inada, T.; Kubo, T. A hydrogen-permselective amorphous silica membrane derived from polysilazane. *J. Eur. Ceram. Soc.* **2005**, 25, 257-264.

⁸ Adhikari, S.; Fernando, S. Hydrogen Membrane Separation Techniques. *Ind. Eng. Chem. Res.* **2006**, 45, 875-881.

⁹ Konegger, T.; Tsai, C. C.; Bordia, R. K. Preparation of Polymer-Derived Ceramic Coatings by Dip-Coating. *Mater. Sci. Forum* **2015**, 825, 645-652.

¹⁰ Sano, S.; Banno, T.; Maeda, M.; Oda, K.; Shibasaki, Y. Slip casting and sintering of silicon carbide. (Part 1): Slip preparation of silicon carbide powder produced by Acheson method. *J. Ceram. Soc. Jpn.* **1996**, 104, 10, 984-988.

¹¹ Ren, Z.; Mujib, S. B.; Singh, G. High-Temperature Properties and Applications of Si-Based Polymer-Derived Ceramics: A Review. *Materials* **2021**, 14, 614.

¹² Klausmann, A.; Morita, K.; Johanns, K.; Fasel, C.; Durst, K.; Mera, G.; Riedel, R.; Ionescu, E. Synthesis and high-temperature evolution of polysilylcarbodiimide-derived SiCN ceramic coatings. *J. Eur. Ceram. Soc.* **2015**, 35, 3771-3780.

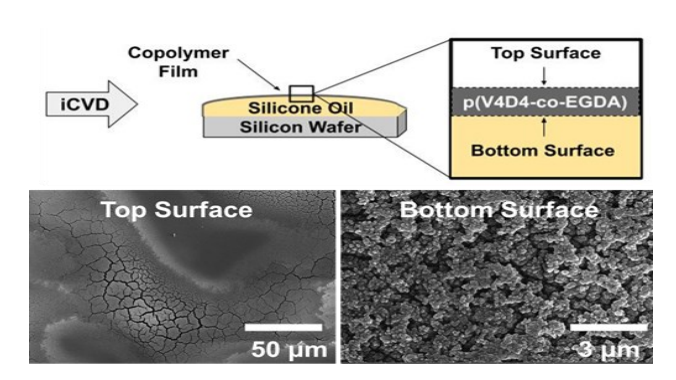
¹³ Hauser, R.; Nahar-Borchard, S.; Riedel, R.; Ikuhara, Y.; Iwamoto, Y. Polymer-Derived SiBCN Ceramic and their Potential Application for High Temperature Membranes. *J. Ceram. Soc. Jpn.* **2006**, 114, 6, 524-528.

¹⁴ Im, S. G.; Gleason, K. K. Solvent-free modification of surfaces with polymers: The case for initiated and oxidative chemical vapor deposition (CVD). *AIChE J.* **2011**, 57, 276-285.

- ¹⁵ Baxamusa, S. H.; Gleason, K. K. Thin Polymer Films with High Step Coverage in Microtrenches by Initiated CVD. *Chem. Vapor Depos.* **2008**, 14, 313-318.
- ¹⁶ Baxamusa, S. H.; Im, S. G.; Gleason, K. K. Initiated and Oxidative Chemical Vapor Deposition: A Scalable Method for Conformal and Functional Polymer Films on Real Substrates. *Phys. Chem. Phys.* **2009**, 11 (26), 5227–5240.
- ¹⁷ Xu, J.; Gleason, K. K. Conformal polymeric thin films by low-temperature rapid initiated chemical vapor deposition (iCVD) using tert-butyl peroxybenzoate as an initiator. *ACS Appl. Mater. Interfaces* **2011**, 3, 2410–2416.
- ¹⁸ Nguyen, B.; Dabir, S.; Tsotsis, T.; Gupta, M. Fabrication of Hydrogen-Selective Silica Membranes via Pyrolysis of Vapor Deposited Polymer Films. *Ind. Eng. Chem. Res.* **2019**, 58, 15190-15198.
- ¹⁹ De Luna, M. M.; Karandikar, P.; Gupta, M. Interactions between polymers and liquids during initiated chemical vapor deposition onto liquid substrates. *Mol. Syst. Des. Eng.* **2020**, 5, 15-21.
- ²⁰ De Luna, M. M.; Karandikar, P.; Gupta, M. Synthesis of Inorganic/Organic Hybrid Materials via Vapor Deposition onto Liquid Surfaces. *ACS Appl. Nano Mater.* **2018**, 1, 6575–6579.
- ²¹ Karandikar, P.; Gupta, M. Synthesis of Functional Particles by Condensation and Polymerization of Monomer Droplets in Silicone Oils. *Langmuir* **2017**, 33, 7701–7707.
- ²² Haller, P. D.; Bradley, L. C.; Gupta, M. Effect of Surface Tension, Viscosity, and Process Conditions on Polymer Morphology Deposited at the Liquid–Vapor Interface. *Langmuir* **2013**, 29, 11640–11645.
- ²³ Haller, P. D.; Gupta, M. Synthesis of Polymer Nanoparticles via Vapor Phase Deposition onto Liquid Substrates. *Macromol. Rapid Commun.* **2014**, 35, 2000–2004.
- ²⁴ Frank-Finney, R. J.; Gupta, M. Two-Stage Growth of Polymer Nanoparticles at the Liquid–Vapor Interface by Vapor-Phase Polymerization. *Langmuir* **2016**, 32, 11014–11020.
- ²⁵ Haller, P. D.; Frank-Finney, R. J.; Gupta, M. Vapor-Phase Free Radical Polymerization in the Presence of an Ionic Liquid. *Macromolecules* **2011**, 44, 2653–2659.
- ²⁶ Karandikar, P.; Gupta, M. Fabrication of ionic liquid gel beads via sequential deposition. *Thin Solid Films* **2017**, 635, 17–22.
- ²⁷ Frank-Finney, R. J.; Bradley, L. C.; Gupta, M. Formation of Polymer–Ionic Liquid Gels Using Vapor Phase Precursors. *Macromolecules* **2013**, 46, 6852–6857.
- ²⁸ Bradley, L. C.; Gupta, M. Microstructured Films Formed on Liquid Substrates via Initiated Chemical Vapor Deposition of Cross-Linked Polymers. *Langmuir* **2015**, 31, 7999–8005.

²⁹ Safo, I. A.; Dosche, C.; Özaslan, M. Effects of Capping on the Oxygen Reduction Reaction Activity and Shape Stability of Pt Nanocubes. *ChemPhysChem* **2019**, 20, 3010-3023.

For Table of Contents Only



³⁰ Bradley, L. C.; Gupta, M. Formation of Heterogeneous Polymer Films via Simultaneous or Sequential Depositions of Soluble and Insoluble Monomers onto Ionic Liquids. *Langmuir* **2013**, 29, 10448–10454.

³¹ Kim, C. H.; Joo, C.; Chun, H. J.; Yoo, B. R.; Noh, D. I.; Shim, Y. B. Instrumental studies on silicone oil adsorption to the surface of intraocular lenses. *Appl. Surf. Sci.* **2012**, 262, 146–152

³² Barton, A. F. M. *CRC Handbook of Solubility Parameters and Other Cohesion Parameters*. Second Edition; CRC Press, **1991**.